

Analysis of the Accuracy of Methods for the Direct Measurement of Emissivity

Raúl B. Pérez-Sáez · Leire del Campo ·
Manuel J. Tello

Published online: 18 March 2008
© Springer Science+Business Media, LLC 2008

Abstract Emissivity measurements are of great interest for both theoretical studies and technological applications. Emissivity is a property that specifies how much radiation a real body emits as compared to a blackbody. The emissivity determination of a sample should be an easy task: a simple comparison between the sample and blackbody radiation at the same temperature. Unfortunately, when measuring the emissivity, some practical problems arise due to the differences between the true emitted radiation and the detected quantity. To clarify this point, an analysis of different direct methods for emissivity measurement is presented. Furthermore, a method that includes multiple reflections is developed. The systematic errors associated with each method are computed theoretically as a function of wavelength, sample temperature, and emissivity, and the surrounding enclosure temperature and emissivity. In general, the error is very high for small sample enclosures, but it strongly decreases when the enclosure area increases. Although at short wavelengths all the analyzed methods produce similar errors, noticeable differences appear under other conditions, and methods considering more radiation terms do not always produce lower errors.

Keywords Direct measurement · Emissivity · Radiometry · Systematic error

R. B. Pérez-Sáez (✉) · L. del Campo · M. J. Tello
Departamento de Física de la Materia Condensada, Facultad de Ciencia y Tecnología,
Universidad del País Vasco, Barrio Sarriena s/n, 48940 Leioa, Bizkaia, Spain
e-mail: raul.perez@ehu.es

R. B. Pérez-Sáez · M. J. Tello
Instituto de Síntesis y Estudio de Materiales, Universidad del País Vasco, Apdo. 644,
48080 Bilbao, Spain

1 Introduction

Emissivity is a property that determines the magnitude of radiation emitted by a real body. This physical magnitude can be measured by direct or indirect methods. The indirect ones are based on measurements of other quantities related to the emissivity, and they can be calorimetric or radiometric. With the direct methods, which are the subject of this article, the emissivity is obtained by comparing the radiation emitted by the sample (S_s) to the radiation emitted by a blackbody (S_{bb}) at the same temperature, under similar geometrical and spectral conditions [1]. Thus, the sample emissivity (ε) can be expressed as

$$\varepsilon = \frac{S_s}{S_{bb}}. \quad (1)$$

From an experimental point of view, the application of this equation can be a complicated task. This is because S_s and S_{bb} depend on the response function of the experimental equipment, and also include the background radiation coming from inside the radiometer. Furthermore, the sample signal (S_s) does not only include the radiation emitted by the sample, but it also takes into account the radiation reflected at the sample surface, which will also depend on the sample emissivity. All these facts make Eq. 1 experimentally useless. To find the appropriate equation for the emissivity determination, S_{bb} and S_s have to be expressed by using all the radiation terms. Thus, the blackbody signal can be written as

$$S_{bb}(\lambda, T_{bb}) = R(\lambda)L(\lambda, T_{bb})A_{bb}F_{bb-d} + S_0(\lambda), \quad (2)$$

where the dependence of the radiation on the wavelength and the temperature is explicitly indicated. $R(\lambda)$ is the response function of the radiometer, and $S_0(\lambda)$ includes all the background radiation that reaches the detector directly, its main component being the radiation coming from the inner parts of the radiometer. A_{bb} is the blackbody area, and F_{bb-d} is the configuration factor [1] between the blackbody and the detector, which gives the fraction of the radiation emitted by the blackbody reaching the detector. We will assume that the temperature of the radiometer remains constant during the experiment, so $R(\lambda)$ and $S_0(\lambda)$ are considered to be temperature independent. It is interesting to remark that most authors [2–6] multiply the $S_0(\lambda)$ term by the response function. Finally, $L(\lambda, T)$ in Eq. 2 represents the radiation emitted by the blackbody, as given by Planck's equation,

$$L(\lambda, T) = \frac{2c_1}{\lambda^5(e^{c_2/\lambda T} - 1)}, \quad (3)$$

where $c_1 = hc^2$ and $c_2 = hc/k$, h is Planck's constant, c is the velocity of light in vacuum, and k is Boltzmann's constant.

In a similar way, the sample signal can be written as

$$S_s(\lambda, T) = R(\lambda)L_s^*(\lambda, T)A_sF_{s-d} + S_0(\lambda), \quad (4)$$

where $L_s^*(\lambda, T)$ is the radiation leaving the sample, which depends on the sample emissivity (ε). A_s is the sample area, and F_{s-d} is the configuration factor between the sample and detector.

On the other hand, $L_s^*(\lambda, T)$ is determined by the radiometer calibration, which basically involves calculating $R(\lambda)$ and $S_0(\lambda)$ [2–6]. The usual way to perform the calibration is to measure the blackbody signal (S_{bb}) at two different temperatures, T_1 and T_2 ,

$$S_{bb1}(\lambda, T_1) = R(\lambda)L(\lambda, T_1)A_{bb}F_{bb-d} + S_0(\lambda) \tag{5a}$$

and

$$S_{bb2}(\lambda, T_2) = R(\lambda)L(\lambda, T_2)A_{bb}F_{bb-d} + S_0(\lambda). \tag{5b}$$

So, the response function $R(\lambda)$ and the background radiation $S_0(\lambda)$ are given by

$$R(\lambda) = \frac{S_{bb2}(\lambda, T_2) - S_{bb1}(\lambda, T_1)}{L(\lambda, T_2) - L(\lambda, T_1)} \frac{1}{A_{bb}F_{bb-d}}, \tag{6}$$

and

$$S_0 = S_{bb2} - R(\lambda)L(\lambda, T_2)A_{bb}F_{bb-d} = S_{bb1} - R(\lambda)L(\lambda, T_1)A_{bb}F_{bb-d}. \tag{7}$$

The preference to consecutively measure the S_{bb1} and S_{bb2} signals must be mentioned, because if the thermal and mechanical stability of the radiometer are not sufficiently good, both $R(\lambda)$ and $S_0(\lambda)$ can vary with time. To avoid errors due to drift of the radiometer properties, each emissivity measurement should include a calibration, that is, $R(\lambda)$ and $S_0(\lambda)$ should be obtained for each emissivity measurement.

This article deals with direct radiometric emissivity measurements of opaque samples. The sample is assumed to be surrounded by an enclosure, for example, a sample chamber. All surfaces are considered to be isothermal, and to emit and reflect diffusely. In Sect. 2, several emissivity measurement methods are analyzed, where different approximations are assumed. In Sect. 3, the systematic errors of the studied methods are compared.

2 Direct Emissivity Measurement Methods

If we take into account that the optical path for the sample and the blackbody is the same, then $A_{bb}F_{bb-d} = A_sF_{s-d}$. With this assumption, we obtain the following expression for $L_s^*(\lambda, T)$ by using Eqs. 4, 6, and 7:

$$L_s^* = \frac{S_s - S_{bb1}}{S_{bb2} - S_{bb1}}(L_2 - L_1) + L_1 = \frac{S_s - S_{bb2}}{S_{bb2} - S_{bb1}}(L_2 - L_1) + L_2, \tag{8}$$

where the dependence on T and λ is not explicitly shown: $L_s^* = L_s^*(\lambda, T)$, $L_1 = L(\lambda, T_{bb1})$, $L_2 = L(\lambda, T_{bb2})$, $S_s = S_s(\lambda, T)$, $S_{bb1} = S_{bb1}(\lambda, T_{bb1})$, $S_{bb2} = S_{bb2}(\lambda, T_{bb2})$.

Equation 8 permits L_s^* to be obtained from the measured signals S_s , S_{bb1} , and S_{bb2} , but if the final aim is to determine the emissivity, we need a functional relation between L_s^* and ε . Among the methods or models that lead to the equation $L_s^* = L_s^*(\varepsilon)$, we have analyzed five, which differ in the way the radiation from the surroundings is taken into account.

2.1 Multiple Reflection Method (multi)

With this method (the most complete approach), L_s^* includes the sample self-emitted radiation, the sample radiation reflected by its surroundings, and the radiation of the surroundings reflected from the sample surface.

(a) Sample self emission

The radiation emitted by the sample that reaches the detector can be written as

$$\varepsilon L_s A_s F_{s-d}, \quad (9)$$

where the dependence on λ and T has not been explicitly indicated to simplify the notation.

(b) Sample emission reflected by the surroundings and reflected back by the sample

Additionally, part of the radiation emitted by the sample, after being reflected by the surroundings and again by the sample, can arrive at the detector. This radiation can be written as

$$\varepsilon L_s A_s F_{s-sur} r_{sur} F_{sur-s} r F_{s-d} = \varepsilon L_s A_s F_{s-d} s \quad (10)$$

where $s = F_{s-sur} r_{sur} F_{sur-s} r$ represents the fraction of the radiation emitted by the sample that has been reflected by the surroundings and reflected back by the sample, $r_{sur} = 1 - \varepsilon_{sur}$ is the reflectivity of the surroundings, and $r = 1 - \varepsilon$ is the sample reflectivity. Furthermore, if multiple reflections occur, not only between the sample and the surroundings, but also between the surroundings with themselves, we will also have to take into account the following terms:

$$\varepsilon L_s A_s (F_{s-sur} r_{sur} F_{sur-s} r)^i (F_{sur-sur} r_{sur})^j F_{s-d} = \varepsilon L_s A_s F_{s-d} s^i t^j, \quad (11)$$

where i and j are integers ($i \geq 1$, $j \geq 0$), and $t = F_{sur-sur} r_{sur}$ represents the fraction of the radiation coming from the surroundings that is reflected by the surroundings. This t factor appears because part of the sample surroundings can receive radiation directly from other parts of the surroundings. $F_{sur-sur}$ is the configuration factor between the surroundings and themselves. The radiation contribution of this section is given by summing all the terms in Eq. 11:

$$\varepsilon L_s A_s F_{s-d} \left[\sum_{i=1}^{\infty} \sum_{j=0}^{\infty} s^i t^j \right] = \varepsilon L_s A_s F_{s-d} \left[\frac{s}{1-s} \frac{1}{1-t} \right]. \tag{12}$$

(c) Surroundings emission reflected at the sample

Finally, L_s^* also includes radiation emitted by the sample surroundings that is reflected by the sample. Thus, the fraction of this radiation that reflects once from the sample and reaches the detector is given by

$$\varepsilon_{sur} L_{sur} A_{sur} F_{sur-s} r F_{s-d} = \varepsilon_{sur} L_{sur} A_s F_{s-sur} r F_{s-d}, \tag{13}$$

where we have used the configuration factor reciprocity relation, $A_{sur} F_{sur-s} = A_s F_{s-sur}$. Furthermore, taking into account that multiple reflections can occur, new terms appear:

$$\varepsilon_{sur} L_{sur} A_s F_{s-sur} r F_{s-d} s^i t^j, \tag{14}$$

where i and j are integers and $i, j \geq 0$. Summing all these terms,

$$\varepsilon_{sur} L_{sur} A_s F_{s-sur} r F_{s-d} \sum_{i=0}^{\infty} s^i \sum_{j=0}^{\infty} t^j = \varepsilon_{sur} L_{sur} A_s F_{s-sur} r F_{s-d} \frac{1}{1-s} \frac{1}{1-t}. \tag{15}$$

Summing Eqs. 9, 12, and 15, the radiation leaving the sample surface that reaches the detector is $A_s F_{s-d} L_s^*$, where

$$L_s^* = \varepsilon L_s \left(1 + \frac{s}{(1-s)(1-t)} \right) + \varepsilon_{sur} L_{sur} F_{s-sur} (1 - \varepsilon) \left(\frac{1}{(1-s)(1-t)} \right), \tag{16}$$

and

$$s = (1 - \varepsilon_{sur})(1 - \varepsilon) \frac{A_s}{A_{sur}} F_{s-sur}^2, \tag{17a}$$

$$t = (1 - \varepsilon_{sur}) \left(1 - \frac{A_s}{A_{sur}} F_{s-sur} \right), \tag{17b}$$

where the configuration factor reciprocity has been used. If $A_s \ll A_{sur}$, some approximations can be made to s and t :

$$\frac{1}{1-s} \approx 1 + s, \quad (s \ll 1), \tag{18a}$$

$$\frac{1}{1-t} \approx \frac{1}{\varepsilon_{sur}} - \frac{r_{sur}}{\varepsilon_{sur}^2} F_{s-sur} \frac{A_s}{A_{sur}}. \tag{18b}$$

Assuming this, Eq. 16 can be written as follows:

$$L_s^* = \varepsilon L_s + F_{s-sur} L_{sur} (1 - \varepsilon) + s \left[\frac{\varepsilon L_s + L_{sur} (F_{s-sur} (1 - \varepsilon) \varepsilon_{sur} - 1)}{\varepsilon_{sur}} \right]. \quad (19)$$

Additionally, we can consider that most of the radiation emitted by the sample is incident on its surroundings, and only a relatively small fraction reaches the detector. Then, F_{s-sur} can be taken as approximately equal to one. Thus,

$$L_s^* = \varepsilon L_s + L_{sur} (1 - \varepsilon) + s \left[\frac{\varepsilon L_s + L_{sur} ((1 - \varepsilon) \varepsilon_{sur} - 1)}{\varepsilon_{sur}} \right]. \quad (20)$$

To evaluate the emissivity, our first task is to obtain L_s^* by using Eq. 8 and then, by using Eq. 16, ε is calculated.

2.2 Single Reflection Method (single)

In the single reflection method [7], the multiple reflections between the sample and the surroundings are neglected, and only a single reflection of the emission from the surroundings at the sample surface is taken into account. Thus, L_s^* has two terms, namely, the direct sample emission and the surroundings emission reflected by the sample:

$$L_s^* = \varepsilon L_s + (1 - \varepsilon) \varepsilon_{sur} L_{sur} F_{s-sur}, \quad (21)$$

where the configuration factor reciprocity relation $A_{sur} F_{sur-s} = A_s F_{s-sur}$ has been used. Then, using Eq. 21, the emissivity is given by

$$\varepsilon = \frac{L_s^* - \varepsilon_{sur} L_{sur} F_{s-sur}}{L_s - \varepsilon_{sur} L_{sur} F_{s-sur}}. \quad (22)$$

Replacing L_s^* by its value (Eq. 8), the emissivity is equal to

$$\varepsilon = \frac{S_s - S_{bb1}}{S_{bb2} - S_{bb1}} \frac{L_2 - L_1}{L_s - \varepsilon_{sur} L_{sur} F_{s-sur}} + \frac{L_1 - \varepsilon_{sur} L_{sur} F_{s-sur}}{L_s - \varepsilon_{sur} L_{sur} F_{s-sur}}. \quad (23)$$

In Eqs. 22 and 23, F_{s-sur} can be taken as equal to one when most of the radiation leaving the sample is incident on the surroundings.

2.3 Black Surrounding Method (blacksur)

In this measurement method, the sample surroundings are considered to be a black enclosure whose emissivity is one; that is, the surroundings are assumed to emit black-body radiation [2, 8, 9]. In this situation, $\varepsilon_{sur} = 1$ and Eqs. 22 and 23 can be written as

$$\varepsilon = \frac{L_s^* - L_{\text{sur}} F_{s-\text{sur}}}{L_s - L_{\text{sur}} F_{s-\text{sur}}}, \quad (24)$$

and

$$\varepsilon = \frac{S_s - S_{\text{bb}1}}{S_{\text{bb}2} - S_{\text{bb}1}} \frac{L_2 - L_1}{L_s - L_{\text{sur}} F_{s-\text{sur}}} + \frac{L_1 - L_{\text{sur}} F_{s-\text{sur}}}{L_s - L_{\text{sur}} F_{s-\text{sur}}}. \quad (25)$$

As previously stated, $F_{s-\text{sur}}$ can be taken as equal to one.

2.4 No Surroundings Method (nosur)

In this method, the radiation from the surroundings is not taken into account ($L_{\text{sur}} = 0$), so L_s^* only includes the term related to the sample emission [10], and

$$\varepsilon = \frac{L_s^*}{L_s}. \quad (26)$$

Using Eq. 8,

$$\varepsilon = \frac{S_s - S_{\text{bb}1}}{S_{\text{bb}2} - S_{\text{bb}1}} \frac{L_2 - L_1}{L_s} + \frac{L_1}{L_s}. \quad (27)$$

2.5 Simple Method (simple)

In this approximation, neither the radiation from the surroundings nor the background radiation $S_0(\lambda)$ is taken into account [11–13], so Eqs. 2 and 4 can be simplified:

$$S_{\text{bb}}(\lambda, T_{\text{bb}}) = R(\lambda) L(\lambda, T_{\text{bb}}) A_{\text{bb}} F_{\text{bb}-d}, \quad (28a)$$

$$S_s(\lambda, T_s) = R(\lambda) L_s^*(\lambda, T_s) A_s F_{s-d}. \quad (28b)$$

Thus, Eq. 8 becomes useless, but using Eq. 28, we obtain

$$L_s^* = \frac{S_s}{S_{\text{bb}}} L_{\text{bb}}, \quad (29)$$

where, again, $A_{\text{bb}} F_{\text{bb}-d} = A_s F_{s-d}$ has been assumed. Furthermore, we use Eq. 26, which is valid for this method, and the emissivity can be obtained as

$$\varepsilon = \frac{S_s}{S_{\text{bb}}} \frac{L_{\text{bb}}}{L_s}. \quad (30)$$

3 Systematic Error Analysis

In this section, the different methods reviewed in the previous section are analyzed. The emissivity obtained by using each method (Eqs. 22, 24, 26, and 30), which will be referred to as the approximate emissivity (ε_{app}), is compared to the emissivity obtained by the most complete method, the multiple reflection method. Thus, the multiple reflection method will be used as the reference in determining the systematic error in the emissivity when using the other methods.

To obtain the approximate emissivity, a theoretical gray emissivity (ε) is assumed for the sample. Using the multiple reflection method (Eq. 16), a theoretical L_s^* is calculated, which is assumed to represent exactly the radiation leaving the sample surface. A sample temperature (T_s), a temperature and a gray emissivity for the surroundings (T_{sur} , ε_{sur}), and a relative area relation for the sample and surroundings enclosure are specified. Once L_s^* is determined, the approximate emissivity is obtained for each method by applying the corresponding equation: Eq. 22 for the single method, Eq. 24 for the blacksour method, Eq. 26 for the nosur method, and Eq. 30 for the simple method. To calculate the approximate emissivity in Eq. 30, S_s and S_{bb} are needed, or experimentally measured $R(\lambda)$ and $S_0(\lambda)$ values can alternatively be used. To use reasonable values, we measured $R(\lambda)$ and $S_0(\lambda)$ for the emissivity measurement setup described in [7]. Blackbody signals at two temperatures were acquired and, applying Eqs. 6 and 7, the response function ($R(\lambda)$) and the background radiation ($S_0(\lambda)$) were calculated. Thus, we have found that the background radiation can be reasonably described as

$$S_0(\lambda) \approx -R(\lambda)L_{315}. \quad (31)$$

It seems that the background radiation is blackbody radiation at $T = 315$ K multiplied by the response function of the radiometer. The minus sign means that the background radiation is an outgoing beam coming from the inner parts of the radiometer and, mainly, from the detector [14]. Thus, this term is not due to incoming radiation that reaches the detector, but to outgoing radiation emitted by the detector itself. According to Eq. 31, this background radiation is approximately equivalent to blackbody radiation at a particular temperature. This can be generalized to any radiometer by denoting this background blackbody temperature as an equivalent temperature (T_{equi}). Taking these assumptions into account, the approximate emissivity calculated by the simple method can be written as follows:

$$\varepsilon_{\text{app}} = \frac{L_{\text{bb}}(L_s^* - L_{\text{equi}})}{L_s(L_{\text{bb}} - L_{\text{equi}})}. \quad (32)$$

To analyze the emissivity errors, we have to take into account that the relative difference (error%) between the real emissivity (the one obtained by the multiple reflection method) and the approximate one, which is given by

$$\text{error}\% = \frac{|\varepsilon - \varepsilon_{\text{app}}|}{\varepsilon} \times 100, \quad (33)$$

is strongly dependent on the measurement conditions: wavelength (λ), sample temperature and emissivity (T_s, ε), surroundings temperature and emissivity ($T_{\text{sur}}, \varepsilon_{\text{sur}}$), ratio of sample and surroundings areas (A_s/A_{sur}), etc. In the next subsections, the influence of these parameters on the errors of each method is analyzed. To simplify the study, in all cases the configuration factor between sample and surroundings ($F_{s-\text{sur}}$) will be considered equal to one.

3.1 Dependence on A_{sur}/A_s and ε_{sur}

First, the influence of the relative surrounding/sample area and the surroundings emissivity on the error of the emissivity is studied for the four approximate methods. The results shown in this section were obtained for a medium wavelength value ($\lambda = 10 \mu\text{m}$) and for a sample emissivity and a surroundings temperature of 0.5 and 295 K, respectively.

The relative error for the four approximate methods has been plotted in Fig. 1 as a function of A_{sur}/A_s for three surroundings emissivities ($\varepsilon_{\text{sur}} = 0.2, 0.6, 0.9$) and two sample temperatures ($T_s = 400$ and 1,000 K). It is clear from Fig. 1 that the systematic error when using the single, blacks, and nosur methods decreases when the relative area A_{sur}/A_s increases. The four methods show a limiting error for high relative area values ($A_{\text{sur}}/A_s \approx 100$), and the emissivity measurement does not improve above this limit. Finally, except for the single method, the limiting error at high A_{sur}/A_s is independent of ε_{sur} .

For the single method (Fig. 1a), the improvement in the emissivity measurement due to the use of a more adequate A_{sur}/A_s ratio does not seem to be effective at low sample temperature and low surroundings emissivity. This means that in this case it is convenient to use highly emitting (i.e., blackbody-like) sample enclosures. For the blacks method (Fig. 1b), the error related to the A_{sur}/A_s ratio is nearly independent of the sample temperature and the surroundings emissivity. Thus, a reasonably large sample enclosure leads to very low error values for this method. For smaller enclosures, it is advisable to use highly emitting surfaces. Comparing the nosur method (Fig. 1c) with the single method (Fig. 1a), we conclude that they have the same qualitative behavior. However, the single method gives higher errors that become unacceptable at low temperature, even using highly emitting enclosures. Finally, for the simple method, the relative error is strongly dependent on the differences between the surroundings and the background equivalent temperature. Figure 1d shows curves for three surroundings temperatures ($T_{\text{sur}} < T_{\text{equi}}, T_{\text{sur}} = T_{\text{equi}}, T_{\text{sur}} > T_{\text{equi}}$), and $T_s = 400$ K. Similar qualitative plots are found for higher sample temperatures. When $T_{\text{sur}} = T_{\text{equi}}$, the error for the simple method decreases to zero with increasing A_{sur}/A_s , but when the difference between T_{sur} and T_{equi} increases, the error does not become zero. Although the simple method neglects all the background radiation, the surprisingly good results for $T_{\text{sur}} = T_{\text{equi}}$ are due to some terms that cancel in Eq. 30. When $T_{\text{sur}} < T_{\text{equi}}$, the approximate emissivity can be overestimated at low values of A_{sur}/A_s and underestimated at high values of A_{sur}/A_s . Thus, the relative error becomes zero at a particular value of A_{sur}/A_s but, since the relative error is positively defined, a singular point appears. This is the case of the curve for $\varepsilon_{\text{sur}} = 0.2$ and $T_{\text{sur}} = 295$ K in Fig. 1d.

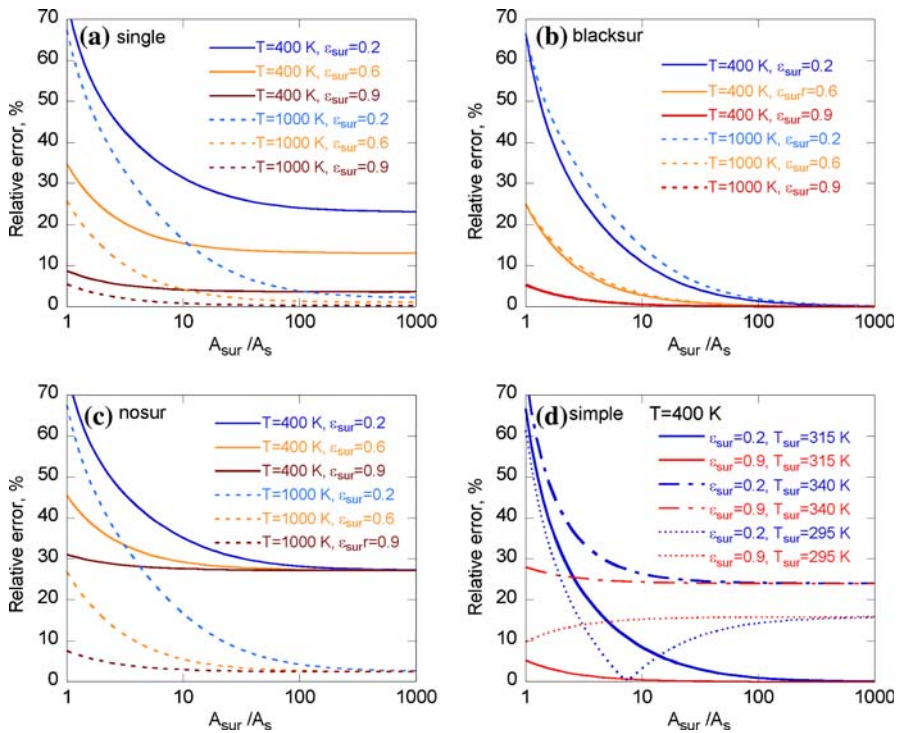


Fig. 1 Relative error as a function of A_{sur}/A_s at two sample temperatures (400 and 1,000 K) and surroundings emissivities (0.2, 0.6, 0.9), for $\lambda = 10 \mu\text{m}$, $\epsilon = 0.5$, and $T_{sur} = 295$ K: (a) single, (b) blacksur, (c) nosur, and (d) simple

Although the relative error at the singular point is zero, it is not possible to use this point to design an ideal experimental setup or to select the best measurement method because the value of A_{sur}/A_s at the singular point depends on the measurement parameters.

Once the dependence on A_{sur}/A_s has been studied, to check the effect of the rest of the parameters, the A_{sur}/A_s ratio will be set to a value of 100 and ϵ_{sur} to 0.95.

3.2 Dependence on λ and T_s

The dependence of the error on the wavelength and the sample temperature is shown in Fig. 2 at low (400 K) and high (1,000 K) temperatures, between 2 and 25 μm , for low and high sample emissivities (0.2 and 0.8), and $T_{sur} = 295$ K.

Figure 2 shows that, for short wavelengths, the relative error is independent of the temperature, but the error is higher for lower emissivities and it decreases when the wavelength decreases and the sample temperature increases. In the case of the blacksur method (Fig. 2b), very low errors are obtained that are almost independent of wavelength and temperature (a slight decrease is observed). The nosur method (Fig. 2c) shows the same qualitative behavior as the single method with λ and T_s , but the error values are much higher for the nosur. Similar behavior, but with higher errors,

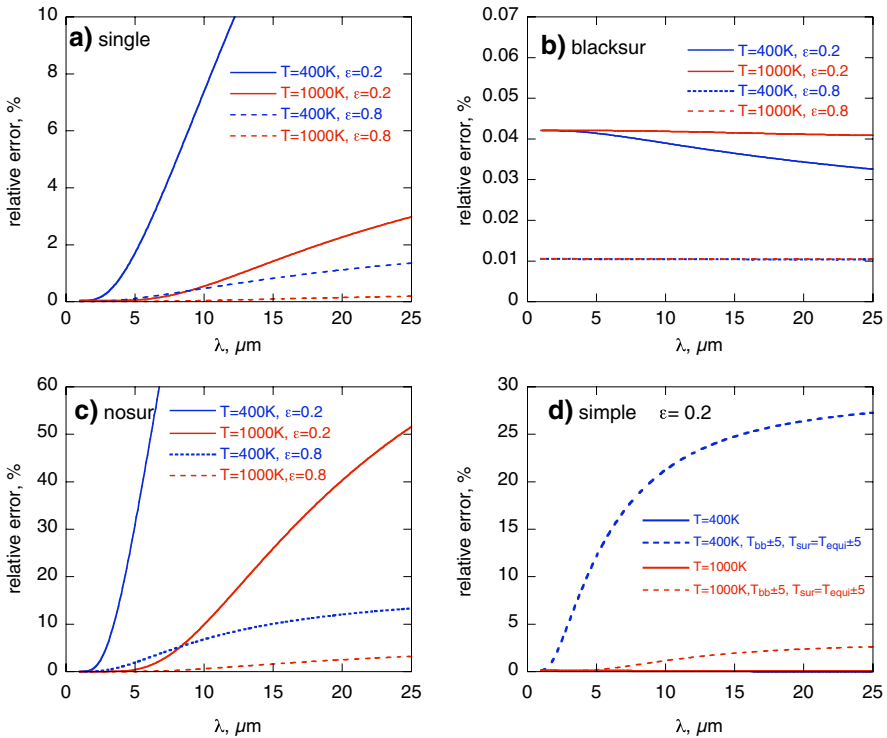


Fig. 2 Relative error as a function of wavelength at two sample temperatures (400 and 1,000 K) and emissivities (0.2, 0.8), for $A_{\text{sur}}/A_s = 100$, $\epsilon_{\text{sur}} = 0.95$, and $T_{\text{sur}} = 295 \text{ K}$: (a) single, (b) blacksur, (c) nosur, and (d) simple

is obtained for lower A_{sur}/A_s ratios and lower ϵ_{sur} values, as already concluded in the previous section.

For the simple method, only the errors for low sample emissivity are shown, but the influence of the differences between the blackbody and sample temperatures, and the differences between the surroundings and equivalent temperatures, are also displayed. Figure 2d shows that the relative error is minimized for $T_{\text{sur}} = T_{\text{equi}}$, and the single method approaches the multiple reflection method. When T_{sur} and T_{bb} are different from T_s and T_{equi} , respectively, the relative error grows. The curves for $T_s - T_{\text{bb}} = 5 \text{ K}$ and $T_{\text{sur}} - T_{\text{equi}} = 5 \text{ K}$ have been plotted in the same figure.

3.3 Dependence on T_{sur}

We will now illustrate the results of the study of the relative errors for each measurement method as a function of the surroundings temperature.

In Fig. 3, three-dimensional plots are shown where the relative error is given as a function of the wavelength and the surroundings temperature for each measurement method, with $T_s = 400 \text{ K}$ and $\epsilon_s = 0.2$. For the single (Fig. 3a) and nosur (Fig. 3c)

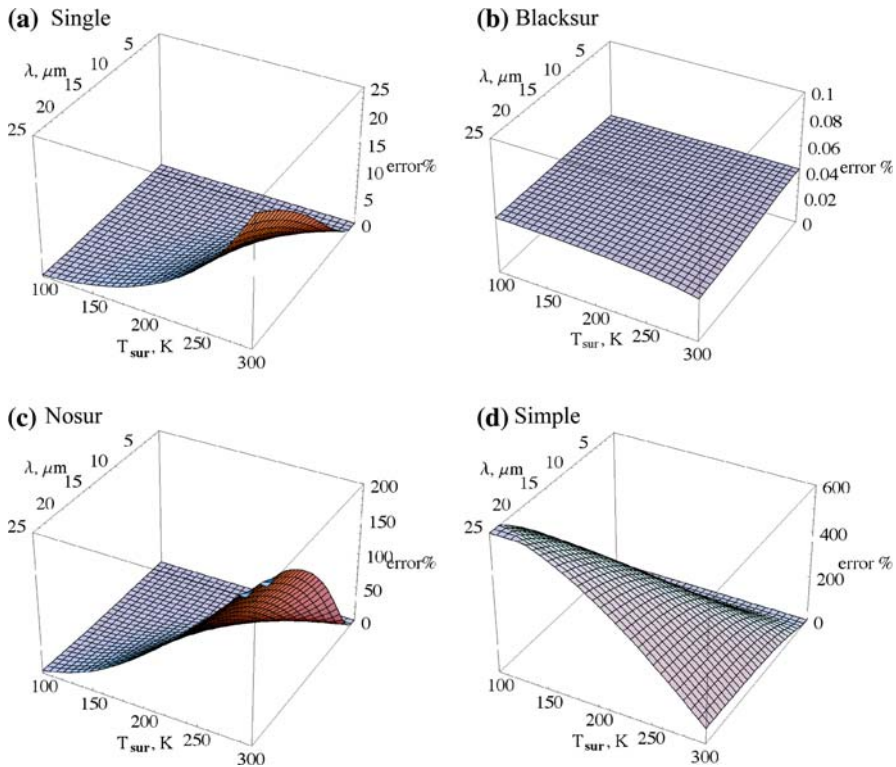


Fig. 3 Three-dimensional plots of the error as a function of the surroundings temperature and between 2 and 25 μm , for $T_s = 400\text{ K}$, $\varepsilon = 0.2$, $\varepsilon_{\text{sur}} = 0.95$, and $A_{\text{sur}}/A_s = 100$: (a) single, (b) blacksour, (c) nosur, and (d) simple

methods, it can be noticed that when T_{sur} decreases ($T_s - T_{\text{sur}}$ increases), the error becomes very low and becomes a constant value, independent of λ . Although both methods show similar qualitative behavior, the error values of the nosur method are much higher. For the blacksour method (Fig. 3b), the error is nearly independent of the surroundings temperature, and its value is low. For the simple method, as observed in Fig. 3d, the relative error strongly increases when the surroundings temperature decreases. This is related to the fact that the error associated with this method is minimized when $T_{\text{sur}} = T_{\text{equi}}$, so when the surroundings temperature differs from the equivalent temperature, the error increases. These results strongly suggest that when using the single and nosur measurement methods, it would be advisable to cool the surrounding enclosure, but this procedure is irrelevant when using the blacksour method. Furthermore, one must avoid cooling the sample enclosure with the simple method.

It is also interesting to check the ability of the four methods to measure the emissivity when the sample temperature is close to the surroundings temperature. In Fig. 4, the relative error is plotted as a function of the sample temperature for two sample emissivities ($\varepsilon_s = 0.2$ and 0.8), short wavelength ($\lambda = 2\ \mu\text{m}$), and $T_{\text{sur}} = 295\text{ K}$. For the single (Fig. 4a) and blacksour (Fig. 4b) methods, as the sample temperature

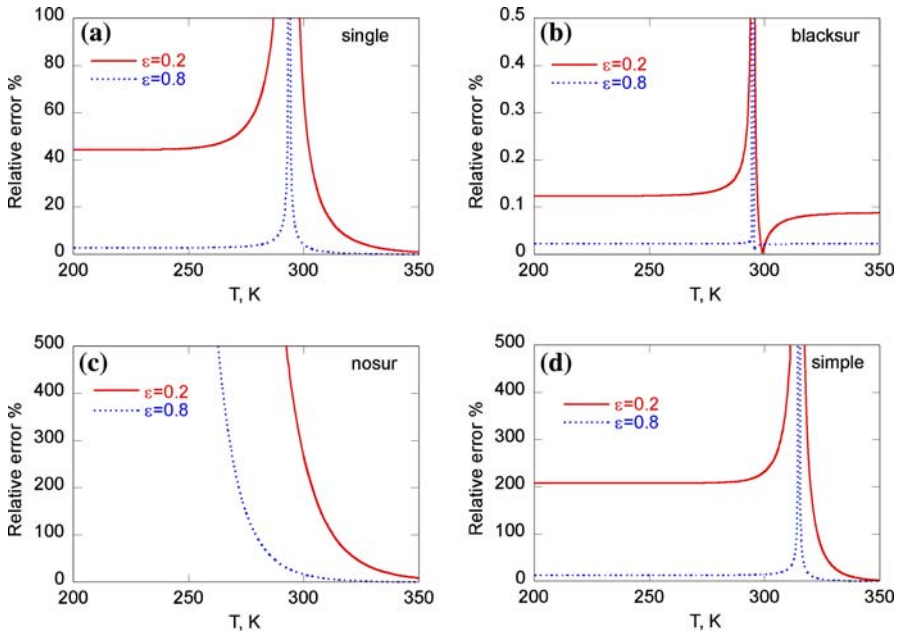


Fig. 4 Relative error as a function of the sample temperature at two sample emissivities (0.2, 0.8), for $\lambda = 2 \mu\text{m}$, $T_{\text{sur}} = 295 \text{ K}$, $\epsilon_{\text{sur}} = 0.95$, and $A_{\text{sur}}/A_s = 100$: (a) single, (b) blacksurr, (c) nosurr, and (d) simple

decreases and its value approaches the surroundings temperature, the error grows, diverging when $T_s = T_{\text{sur}}$. For $T_s < T_{\text{sur}}$, once the two temperatures are sufficiently separated, the emissivity error decreases but, for the single method, the error can be unacceptably high, especially for low emissivity samples. The blacksurr method leads to satisfactory enough results even very near the surroundings temperature. As shown in Fig. 4c, for the nosurr method, when the sample temperature decreases and approaches the surroundings temperature, the error monotonically increases. Figure 4d, where $T_{\text{equi}} - T_{\text{sur}} = 5 \text{ K}$, shows the behavior of the simple method, which is qualitatively similar to that of the single and blacksurr methods, although the diverging temperature is not the surroundings temperature but the equivalent one ($T_{\text{equi}} = 315 \text{ K}$). In this case, for $T_s < T_{\text{sur}}$, the error can be even higher than for the single method.

3.4 Final Discussion

To better compare the studied emissivity measurement methods, we plot in Fig. 5 the relative error for the analyzed methods as a function of wavelength for two sample temperatures (400 and 1,000 K) and emissivities (0.2 and 0.8). As before, the surroundings emissivity and temperature have been set to $\epsilon_{\text{sur}} = 0.95$, $T_{\text{sur}} = 295 \text{ K}$, and $A_{\text{sur}}/A_s = 100$. For the simple method, the blackbody temperature is assumed to be equal to the sample temperature, and curves for $T_{\text{equi}} - T_{\text{sur}} = 5$ and 20 K are displayed. As observed in Fig. 5, in all the cases, the four compared methods have

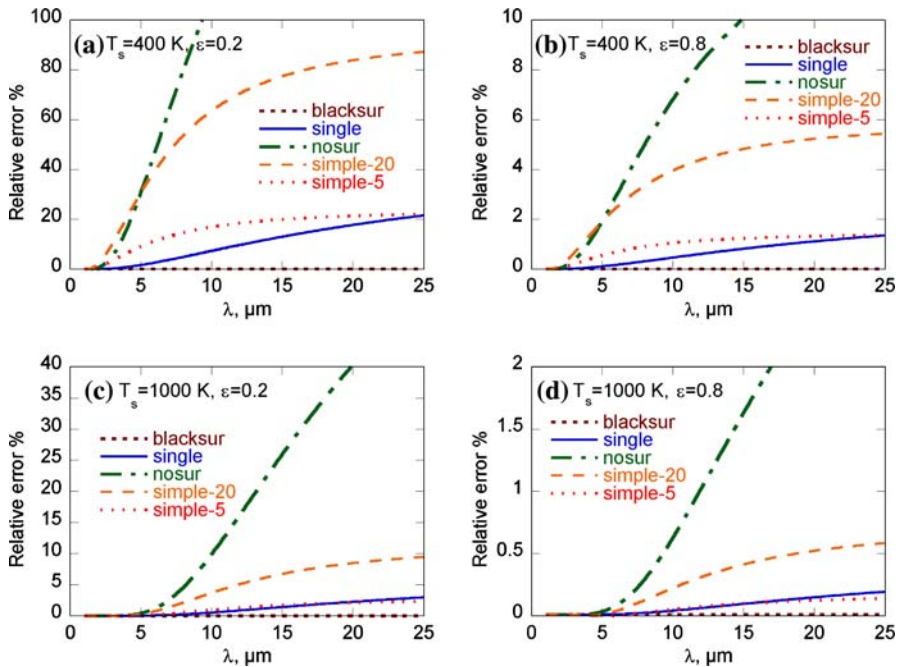


Fig. 5 Comparison between the emissivity measurement methods at two sample temperatures and emissivities for $T_{\text{sur}} = 295 \text{ K}$, $\varepsilon_{\text{sur}} = 0.95$, and $A_{\text{sur}}/A_s = 100$: (a) $T_s = 400 \text{ K}$ and $\varepsilon = 0.2$, (b) $T_s = 400 \text{ K}$ and $\varepsilon = 0.8$, (c) $T_s = 1,000 \text{ K}$ and $\varepsilon = 0.2$, and (d) $T_s = 1,000 \text{ K}$ and $\varepsilon = 0.8$

the same error for short wavelengths, and the lowest errors are achieved for high temperatures and emissivities.

The worst emissivity measurement method is the nosur one, though surprisingly it makes use of fewer approximations than the simple one. The simple method can lead to satisfactory results, but one should make sure that the surroundings temperature is close to the equivalent temperature, and that the sample and blackbody temperatures are nearly the same. Even though this method tries to correct the differences between the sample and blackbody temperatures, it does so incompletely. It should be remarked that the other methods do not present this problem; that is, their results do not depend on the difference between the sample and blackbody temperatures. One can conclude that, sometimes, the simple method can be a very appropriate emissivity measurement method, but accurate control of the blackbody temperature and the surroundings temperature is necessary. If one cannot know or control these temperatures, it is advisable to use other methods. The single method gives good results over almost the whole wavelength, temperature, and emissivity ranges, when using a highly emitting enclosure. Furthermore, these results can improve by using a cooled sample enclosure. The best-suited method for emissivity measurements is the blacksur one, which gives very low errors, independent of the surroundings emissivity, but large enclosures are necessary. It is remarkable that the blacksur method, which makes more approximations than the simple method, produces better results. This can be explained taking into account

that when $A_s \ll A_{\text{sur}}$, the multiple reflection method (Eq. 20) tends to the blacksur method (Eq. 21) with $\varepsilon_{\text{sur}} = 1$.

Acknowledgments This work has been carried out with the financial support of the SAIOTEK program (Project Number AE03UN01) of the Basque Government, and the “Universidad-Empresa” program (Project Numbers UE03/A14 and UE06/01) of the Basque Country University in collaboration with “Industria de Turbo Propulsores S.A”. L. del Campo gratefully acknowledges the Basque Government for its support through a Ph.D. fellowship.

References

1. R. Siegel, J. Howell, *Thermal Radiation Heat Transfer*, 4th edn. (Taylor and Francis, Washington, 2002)
2. J. Ishii, A. Ono, *Meas. Sci. Technol.* **12**, 2103 (2001)
3. J. Dai, X. Wang, G. Yuan, *J. Phys. Conf. Ser.* **13**, 63 (2005)
4. E. Lindermeier, P. Haschberger, V. Tank, H. Dietl, *Appl. Opt.* **31**, 4527 (1992)
5. H.E. Revercomb, H. Buijs, H.B. Howell, D.D. LaPorte, W.L. Smith, L.A. Sromovsky, *Appl. Opt.* **27**, 3210 (1988)
6. A. Shimota, H. Kobayashi, S. Kadokura, *Appl. Opt.* **38**, 571 (1999)
7. L. del Campo, R.B. Pérez-Sáez, X. Esquisabel, I. Fernández, M.J. Tello, *Rev. Sci. Instrum.* **77**, 113111 (2006)
8. V. Fonseca, Evolution de la liaison chimique dans la phase ferroélectrique de LiNbO3 déterminée par spectroscopie d'émission infrarouge jusqu'à 1550 K. Ph.D. Thesis, Université d'Orléans, 2000
9. J. Manara, R. Caps, H.P. Ebert, F. Hemberger, J. Fricke, *High Temp. High Press.* **34**, 65 (2002)
10. P.C. Dufour, N.L. Rowell, A.G. Steele, *Appl. Opt.* **37**, 5923 (1998)
11. M.J. Ballico, T.P. Jones, *Appl. Spectros.* **49**, 335 (1995)
12. R.M. Sova, M.J. Linevsky, M.E. Thomas, F.F. Mark, *Infrared Phys. Technol.* **39**, 251 (1998)
13. R. Lopes, A. Delmas, J.F. Sacadura, *High Temp. High Press.* **32**, 369 (2000)
14. L. del Campo, Diseño, construcción y calibración de un radiómetro para medir emisividad espectral direccional. Aplicación a materiales de interés tecnológico. Ph.D. Thesis, University of the Basque Country, 2007